Journal Homepage: -www.journalijar.com

INTERNATIONAL JOURNAL OF ADVANCED RESEARCH (IJAR)

Article DOI:10.21474/IJAR01/15688
DOI URL: http://dx.doi.org/10.21474/IJAR01/15688

RESEARCH ARTICLE

PROPERTIES OF MAGNETIC CARBON BASE ON RICINODENDRONHEUDELOTII AND APPLICATION IN REMOVAL OF METHYLENE BLUE

Kouakou Yao Urbain[1], Kambire Ollo[1] and ZranVanh Eric- Simon[2]

1. UFR Sciences Et Technologies, Université de Man, BP 20 Man, Côte d'Ivoire.
2. UFR SSMT, Laboratoire de Constitution et Réaction de la Matière, Université Félix Houphouët-Boigny, 22 BP 582 Abidjan 22, Côte d'Ivoire.

Manuscript Info

Manuscript History
Received: 15 September 2022
Final Accepted: 19 October 2022
Published: November 2022

Key words:-
Magnetic Activated Carbon, RicinodendronHeudelotiiShells, Dye Treatment, Adsorption Kinetics, Fenton Process, Isotherm

Abstract

The shells of RicinodendronHeudelotii, an agricultural waste, were used to prepare magnetic activated carbon. To do this, activated carbon was prepared by chemical activation with NaOH. By co-precipitation with iron II and iron III ions, magnetic carbon (MG-AC) is obtained. These materials were characterized using scanning electron microscopy (SEM), nitrogen gas adsorption measurements at -196°C, energy dispersive X-ray fluorescence and a vibrating sample magnetometer. The results showed that MG-AC had 86.5% Fe_2O_3 and higher magnetic properties with a magnetic saturation of 75 $emu.g^{-1}$. The Brunauer−Emmett−Teller (BET) surface area and pore volume of MG-AC were determined as 86.52 $m^2.g^{-1}$and 0.168 $cm^3.g^{-1}$ respectively. The removal of methylene blue on these two materials (AC and MG-AC) was done in the absence and in the presence of hydrogen peroxide. In the absence of H_2O_2, methylene blue adsorbs on these materials according to a pseudo order 2 kinetics with rates of 0.0047 and 0.0039 $g.mg^{-1}.min^{-1}$ respectively for AC and MG-AC. This adsorption can be described by the Langmuir model with maximum adsorption amounts of 13.4 and 9.6 $mg.g^{-1}$ respectively for AC and MG-AC. The addition of H_2O_2leads to the production of hydroxyl radicals thanks to the presence of iron on MG-AC. Over 4 cycles of use Activated Carbon based on RicinodendronHeudelotii removed 99.6% of MB in the 1st cycle and only 5.23% due to the considerable loss of mass, while MG-AC removed this dye at 94.6% in the first cycle and 68.44% in the 4th cycle. There is therefore less loss of mass during the regeneration of MG-AC which still remains efficient after 4 cycles.

Introduction:-

The presence of certain toxic substances such as dyes in wastewater poses serious environmental problems. Indeed, dyes can be the cause of eutrophication phenomena and be a threat to human and animal health (Aboet al., 2021, Boujaady et al., 2013). There are many means used to remove dyes from water. Ozonation(Suphitchaet al., 2013), electrochemical methods(Ammar et al., 2022, Manoel et al., 2016), advanced oxidation processes (Süheyda et al., 2015)as well as adsorption on various materials including activated carbons (Kambiré et al., 2021, Kouakou et al., 2022) are used for the elimination of various dyes. Among these methods, adsorption on activated carbon has the

Corresponding Author:- Kouakouyao Urbain
Address:- UFR Sciences Et Technologies, Université De Man, BP 20 Man, Côte d'Ivoire.

advantage of being simple, economical and efficient (Sudheer et al., 2020). Indeed, activated carbons have high adsorption efficiency, large surface area, high porosity structure, and high surface reactivity (Seyedehmaryam et al., 2020). The other advantage lies in obtaining activated carbons. These materials are obtained from plant and animal residues containing significant carbon fractions. Thus activated carbons made from corn cobs(Abo et al., 2021), olive dates (Marina et al., 2021), rice husks (Khu et al., 2014), coffee husks (Luiz et al., 2009)have been used to remove dyes from wastewater. Disadvantage of the use of these materials, lies in the difficulty of recovering them after use. One of the promising solutions consists in embedding magnetic oxides in the activated carbons. This process gives carbon the quality of composite nanomaterials with various properties (Water et al., 2014). By combining the adsorption capacity of activated carbon with magnetic iron oxide nanoparticles, a promising material is obtained which has the advantage of being able to be separated from the water in which it is suspended by means of magnetic separators. This technic allows to increase the capacity of the material and its age for long-term use. This new type of adsorbent called magnetic nano-adsorbent not only demonstrated high adsorption efficiency due to its large surface to volume ratio, but also showed additional advantages like ease of synthesis, easy recovery, the absence of secondary pollutants, cost effectiveness and environmental friendliness (Gupta et al., 2012). Magnetic activated carbons are obtained by chemical or physical process. MG-AC is developed by chemically or physically dispersing magnetic particles on the surface of porous AC (Chinedum et al., 2017). The hydrothermal synthesis method, simultaneous activation and magnetization as well as the magnetization of previously activated carbons are the most used (Muslemet al., 2019). The last process requires having activated carbons available. Commercial activated carbons are expensive due to the use of carbon which is an expensive material. One of the solutions is the use of agricultural waste (Panagiota et al., 2008). It is estimated that between 7 and 10 billion tonnes of waste are produced worldwide, including more than 2 billion tonnes of domestic solid waste (Francesca et al., 2019). RicinodendronHeudelotii shells appear as a solution. Indeed, previous work has proven that these shells are excellent precursors for producing activated carbon (Kouakouet al., 2013). The RicinodendronHeudelotii plants give fruits whose kernels are widely used in cooking in Africa and for cosmetics. After extraction of the kernels, the shells which constitute 71% of the whole seeds are thrown away (Kristina et al., 2013). These shells become domestic solid waste since they are not biodegradable. Using this abundant waste material could help to reduce the cost of producing activated carbons.

The objectives of our work are: (1) Prepare activated carbon from RicinodendronHeudelotii (RH) shells by chemical activation, (2) Synthesize magnetic activated carbon from RicinodendronHeudelotii activated carbon and characterize it, (3) eliminate methylene blue (a dye) in water by the use of magnetic activated carbon, then to evaluate the performance and stability of this material.

Materials And Methods:-

Synthesis of materials

Precursor

The shells of RicinodendronHeudelotii used in this work were obtained from peasant women in the city of Bangolo in western Côte d'Ivoire, located 434 km from Abidjan, the capital. After extraction of the almonds for various uses, these shells are abandoned in nature and constitute abundant waste. The shells were first washed with distilled water to remove all impurities, and then dried in an oven at 105 °C for 24 hours. The shells were subsequently crushed to have diameters between 1 and 2 mm.

Figure 1. Photo of shells of RicinodendronHeudelotii.

Chemical agents and equipment

All chemicals used are analytical grade. These are sodium hydroxide supplied by AnalarNormapur VWR Chemicals (Czech Republic), ammonia from Germineo (France), iron II sulphate supplied by Nabta (China), iron III chloride, Sordalab (France) and ultrapure water. The main devices used for the synthesis are: a Nabertherm West Germany muffle furnace and a TCN-115 drying oven.

Material Synthesis Method:-

The preparation of the materials took place in two stages. The first step was to prepare the activated carbon. To do this, the previously cleaned shells of RicinodendronHeudelotii were impregnated with sodium hydroxide NaOH 2 M for 24 hours at 150 rpm. The mixture is filtered and dried in an oven at 105° C for 4 hours. The impregnated shells are then calcined at 500° C in a Nerbatherm muffle furnace (West Germany) under an inert atmosphere with nitrogen for one hour. The activated carbon (AC) obtained is cooled, washed to neutral pH, then dried. The second step consisted in encrusting the activated carbon with iron nanoparticles. To do this, 10g of hydrated iron chloride ($FeCl_3, 6H_2O$), 5 g of hydrated iron sulfate ($FeSO_4, 7H_2O$) and 50 mL of 5 M NaOH were added to 25 g of AC.

This impregnation of the materials follows the following protocol:

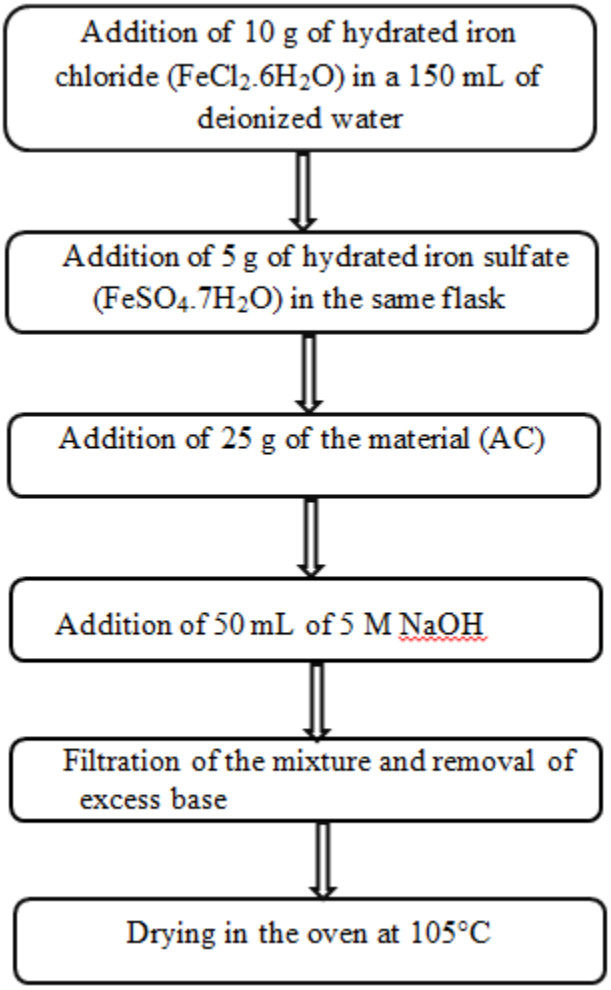

Figure 2:- Steps in the Synthesis of Magnetic Materials.

Characterization of materials

Activated carbon (AC) and magnetic activated carbon (MG-AC) were characterized using Hirox SH-4000 scanning electron microscopy (SEM).Nitrogen gas adsorption measurements were performed at -196°C by using a micromeriticstristar II plus instrument. A HORIBA scientific MESA-50 device was used for the X-ray fluorescence

analysis. The ash content of material was determined by reference to American Standards Technology Method (ASTM), ASTM D 2866-94 (Kouakou et al., 2022). A vibrating sample magnetometer (VSM, Lakeshore, model 7400 series) was used at room temperature and the magnetic response was studied using a squid magnetometer (MPMS, Evercool, 7 T Squid instrument provided by Quantum Design). Finally, bar magnets were used for magnetization tests.

Kinetic study of adsorption and elimination by heterogeneous Fenton of methylene blue

The study of the adsorption kinetics of methylene blue was carried out at room temperature on AC and AC-MG. The objective is to determine the time required to reach the adsorption equilibrium of methylene blue (MB) on each of the materials and the order of the kinetics. For this study, 0.1 g of material was mixed with 50 mL of MB to 25 $mg.L^{-1}$ of solution in a 100 mL conical flask. These mixtures were agitated regularly on a magnetic stirrer at 150 rpm for time intervals of 5 and 120 minutes. After each contact time, the solutions were filtered and the initial and final concentrations of MB were determined by the UV-30 Scan spectrophotometer. The quantity of MB adsorbed per gram of material at time t is expressed by the Equation

$$q_t = \frac{(C_o - C_t)}{m} \times V \quad (1)$$

Where q_t ($mg.g^{-1}$) is the amount of MB adsorbed by AC or MG-AC ; C_0 and C_t are respectively the initial and the final concentration of MB at time after filtration ($mg.L^{-1}$); V (L) is the initial solution volume and m(g) is the mass of the activated carbon or magnetic active carbon.

Regarding the kinetic study of the elimination of MB by heterogeneous Fenton, it is similar to the kinetics seen previously except that here, we added to the mixture a volume of 0.5 mL of hydrogen peroxide

Adsorption of MB on materials and elimination by the heterogeneous Fenton process.

In order to determine the quantities of MB adsorbed according to the type of material, at equilibrium time, we studied the influence of the concentration of the adsorbate. In this case, the study is carried out by varying the initial concentration of MB from 5 $mg.L^{-1}$to 50 $mg.L^{-1}$. A mass of 0.1 g of material is brought into contact with 25 mL of the MB solution of different concentrations [5 $mg.L^{-1}$; 10 $mg.L^{-1}$; 20 $mg.L^{-1}$; 30 $mg.L^{-1}$; 40 $mg.L^{-1}$; 50 $mg.L^{-1}$]. The mixture is stirred regularly at 250 rpm using a magnetic stirrer until equilibrium time. Centrifugation for the separation of material and adsorbate is carried out for 10 minutes using a centrifuge (Mega Star 600). Residual centrifugal concentrations are determined using a UV-30 Scan spectrophotometer.

The amount of MB adsorbed per gram of material at equilibrium is given by the relationship:

$$q_e = \frac{(C_o - C_e)}{m} \times V \quad (2)$$

Where C_0 and $C_e$are the concentrations of MB at initial and equilibrium times, respectively ($mg.L^{-1}$); V is the initial solution volume (L); and m is the mass of AC or MG-AC used (g).

The removal of MB by heterogeneous Fenton is similar to the previous study, except for the addition of 0.5 mL of hydrogen peroxide in this last study.

Stability and performance of materials

In a beaker containing 0.5 g of material, we added 25 mL of methylene blue with a concentration of 100 mg/L. The mixture is stirred regularly at 250 rpm using a magnetic stirrer until equilibrium time. After centrifugation, the supernatant is analyzed by UV spectrophotometer in order to determine the residual concentration.

The percentage removal of methylene blue is given by the formula:

$$\%E = \frac{(C_0 - C_e)}{C_0} \times 100 \quad (3)$$

Where, C_0 and $C_e$are the concentrations of Methylene blue at initial and equilibrium times, respectively ($mg.L^{-1}$). After filtration, the material is recovered, and then washed with distilled water. After this process, the material is again treated with ammonia, then washed with distilled water and finally dried in an oven for 10 hours at 105° C.

After recovery of the material, it is weighed then reused according to the previous protocol. Each of the materials synthesized as part of this study are used and then recycled and reused for 4 cycles.

Results and Discussion:-

Characterization of AC and MG–AC

The purpose of the SEM examination is to illustrate porosity, especially that created by activation. A developed porosity makes it possible to increase the specific surface of the carbon and, consequently, the number of active sites on which the adsorbates can possibly bind. Figure 3 shows heterogeneous surfaces for the two materials. The pores are more developed and open for activated carbon (Fig 3a). On the surface of the MG-AC (Fig 3b), an iron particle cover is observed which can lead to a possible reduction in the surface of the material as well as the volume of the pores. This decrease in surface area results from a random diffusion of iron nanoparticles through the pores of the material (Chinedum et al., 2017). The MG-AC spectrum revealed the actual presence of iron on the carbon surface.From the EDX graph of MG-AC (Fig 3c) the sample was rich in carbon, Oxygen, Fe and Na while the other elements were found in traces.

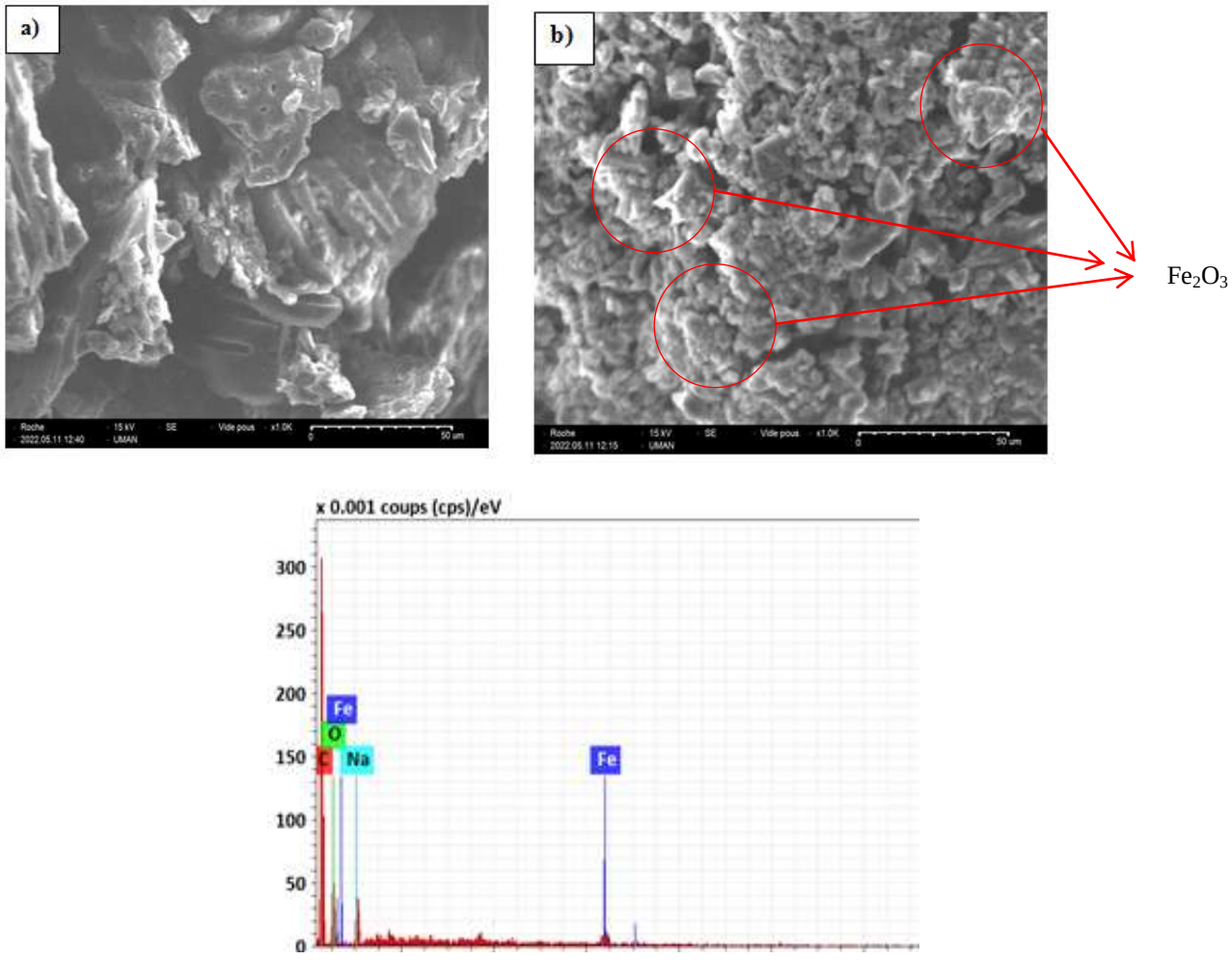

Figure 3:- a) SEM of AC, b) SEM of MG-AC, c) Spectrum of MG-AC

Fluorescence analysis was performed on the magnetic carbon to primarily determine its oxide composition. The result is presented in Figure 4. The material contains more than 86% iron oxide (Fe_2O_3). In view of these results we can say that the material has high magnetic properties, therefore capable of attracting a magnet.

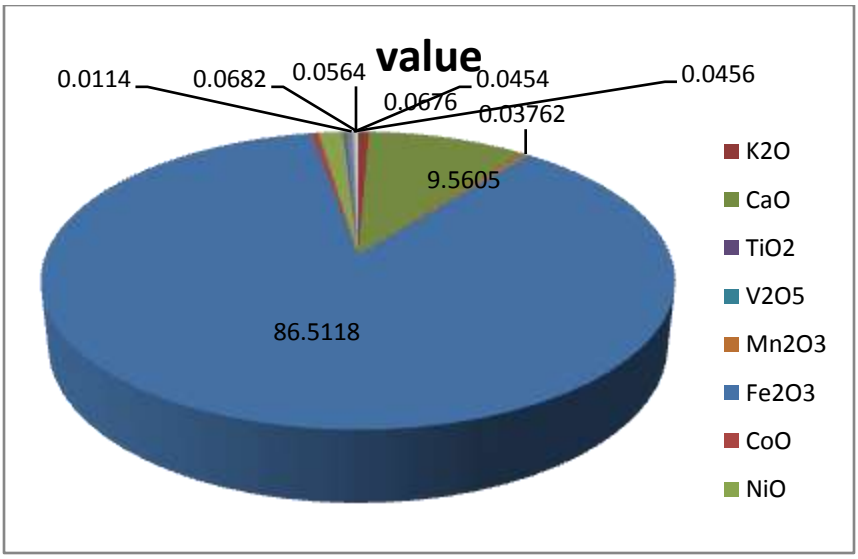

Figure 4:- Oxide percentage of MG-AC.

The ferromagnetic characterization was done with a simple vibration magnetometer. Figure 5 shows the hysteresis plots of the magnetic activated carbon synthesized. The hysteresis free magnetization curve indicating that MG-AC was superparamagnetic. The magnetization strength was 75 emu/g for the MG-AC. Direct use of a bar magnet yielded the results in Figure 6. We see that there is attraction between the bar magnet and the iron-embedded activated carbon (MG-AC). The AC not being impregnated with iron shows no attraction with the magnet. The result of the action of the magnet on the materials shows us that the synthesized MG-AC material is indeed ferromagnetic.

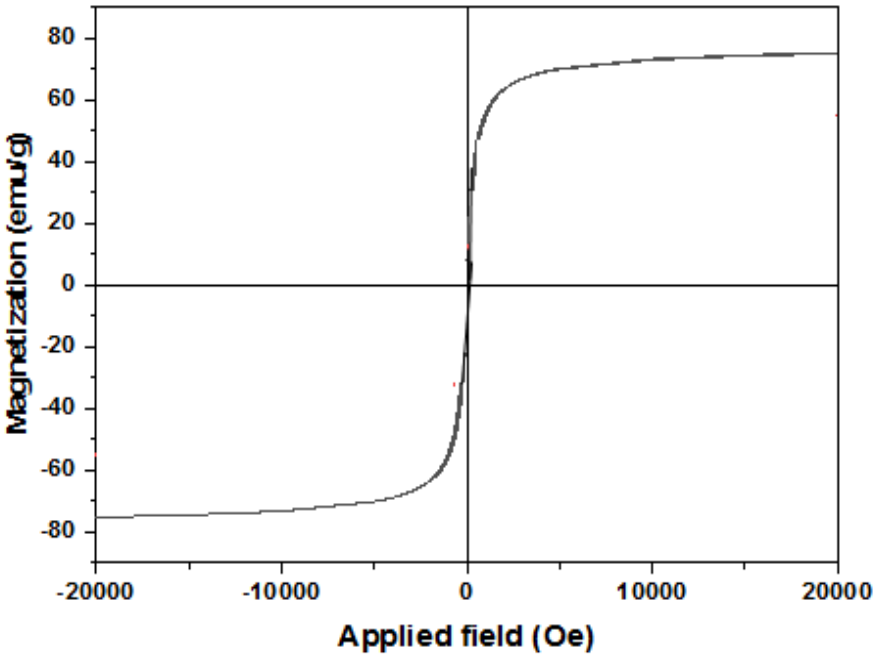

Figure 5. The hysteresis plots of MG-AC.

Figure 6:- Images of the action of the bar magnet on the synthesized materials.

Material properties are summarized in Table 1.The low values of ash content reflect good preparation of the materials. In addition, the specific surface area of AC is greater than that of MG-AC. This may be due to iron oxides clogging certain pores.

Table 1:- Materials properties.

Material	Magnetic saturation (emu.g^{-1})	Surface area S_{BET} (m^2.g^{-1})	Pore volume (cm^3.g^{-1})	Ash content (%)
AC	0	112.31	0.265	5.6
MG-AC	75	86.52	0.168	3.2

Adsorption of methylene blue

Kinetic study of adsorption

Knowledge of the equilibrium time on the elimination of the dye is necessary for the establishment of kinetic models and the determination of isotherms. The curves of the adsorption kinetics (Fig 7) show that for each material, the concentration of MB decreases rapidly during the first 20 minutes. This could be explained by the availability of active sites at the beginning of the experiment. After 20 min, the concentration decreases more or less rapidly, due to the diffusion of MB in the pores. Equilibrium is reached after 90 min for each material. MB adsorption is better on AC than on MG-AC. Indeed, iron particles occupy certain activated sites and thus reduce the adsorption capacity of MG-AC (Urbain et al., 2013). In order to determine the mechanism of adsorption, 3 kinetic models were applied. In this purpose, 3 kinetic models including the pseudo-first-order equation, the pseudo-second-order equation, and intraparticle diffusion model (Ho et al., 1999)were tested here to find out adsorption mechanism:

$ln(q_e - q_t) = lnq_e - k_1 t$ (4)

$\frac{t}{q_t} = \frac{1}{k_2 {q_e}^2} + \frac{1}{q_e} t$ (5)

$q_t = k_i t^{1/2} + c$ (6)

Where$q_t and q_e$ are the amount of MB adsorbed at time t and at equilibrium respectively in (mg/g), t is the contact time in (min), k_1, k_2 and $k_i$are the pseudo first-order reaction rate constant of adsorption of MB on material, the rate constant of the pseudo-second-order model and the rate constant of the intraparticle diffusion respectively and c is the intersection of the line with the axis of ordinates provides information on the thickness of the boundary layer of intraparticle diffusion model.

To evaluate the applicability of these models, we have plotted $ln(q_e - q_t) versus t$ for the pseudo-first-order reaction, $\frac{t}{q_t} versus t$for the pseudo-second-order reaction and $q_t versus t^{1/2}$ for the intraparticle diffusion reaction. The representations of the curves where made it possible to determine the parameters of these models. The values of k_1, $qe_{,cal1}$, R_1^2 (correlation coefficient for pseudo-first order adsorption kinetics), k_2, $qe_{,cal2}$, R_2^2 (correlation coefficient for pseudo-second order adsorption kinetics) and k_i , c, R_i^2 (correlation coefficient for intraparticle diffusion model) were calculated and summarized in Table 2. According the values from this table, the model of pseudo second order with a good correlation coefficient (R_2^2 between 0.9813 and 0.9932) is suitable to describe the

adsorption kinetic of MB onto AC and MG-AC. The applicability of this model suggests that the limiting step in the BM adsorption process on these materials could be chemisorption (Ho et al., 1999).In this mechanism, the kinetics of sorption should correspond to a reversible second order reaction at low sorbate/sorbent ratios (first order at very low ratios), and two competitive reversible second order reactions at higher sorbate/sorbent ratios. This result is consistent with the adsorption of methylene blue on graphene oxides and carbon nanotubes (Yanhui et al., 2013).

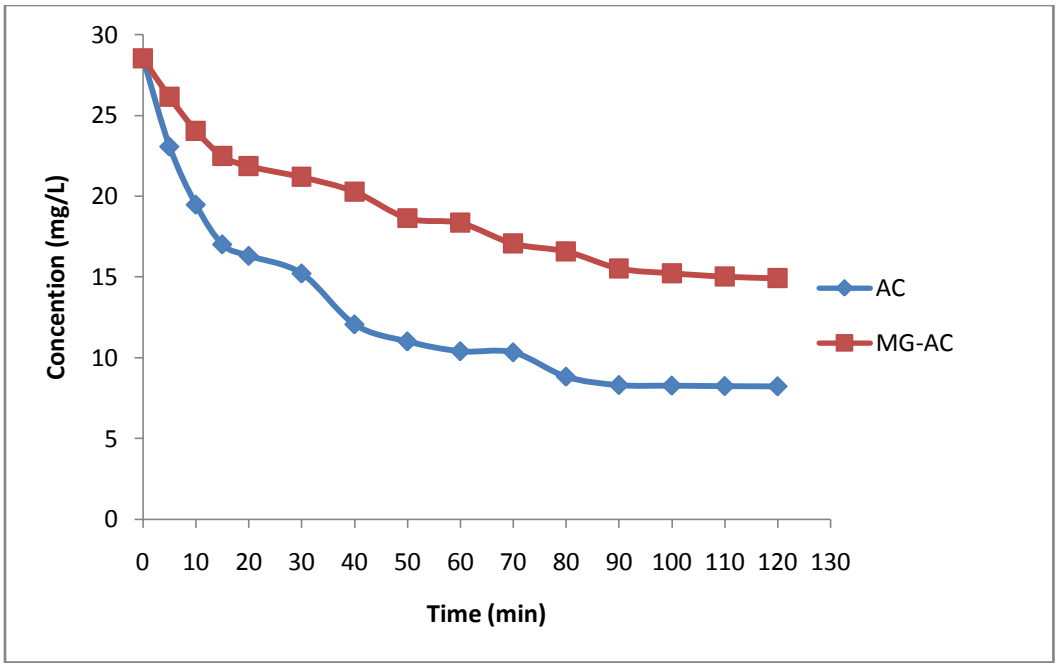

Figure 7:- Evolution of MB as a function of time (Conditions: mass of AC = mass of MG-AC= 0.1 g; T = 25°C).

Table 2:- Values of parameters of the three applied kinetics models for MB adsorption.

	Pseudo-first order			**Pseudo-second order**			**Intraparticle diffusion**		
	k_1(min^{-1})	$qe_{,cal1}$(mg/g)	R_1^2	k_2(g/mg.min)	$qe_{,cal2}$(mg/g)	R_2^2	k_i(mg/gmin$^{1/2}$)	c	R_i^2
AC	0.0382	9.0904	0.9495	0.0047	11.8624	0.9932	1.0416	0.9017	0.9641
MG-AC	0.0284	6.1367	0.9715	0.0039	8.2101	0.9813	1.2939	2.2495	0.9488

Study of adsorption at equilibrium

The study of the adsorption of MB on AC and MG-AC was carried out at 25°C. The amount of dye adsorbed at equilibrium per mass of material is given in Figure 8. The amount of MB adsorbed increase with the concentration at equilibrium. These isotherms appear to be type I according to the IUPAC classification, justifying the microporous aspect of AC and MG-AC (Fig 8.a). The percentage removal of methylene blue increases with concentration (Fig 8.b). This is justified that with increasing concentration, the amount of adsorbent increases.

To study the adsorption phenomenon, 2 models were used namely the Freundlich model and the Langmuir model (Oualid et al., 2007).

The empirical Freundlich equation is written:

$$q_e = K_F C_e^{1/n} \qquad (7)$$

C_e (mg/L) is the concentration of MB at equilibrium in the residual solution, K_F[(mg/g)(L/mg)$^{\frac{1}{n}}$] andn (unitless) are Freundlich's.

The Langmuir equation is written:

$$q_e = \frac{q_m b C_e}{1+bC_e} \qquad (8)$$

With b the Langmuir thermodynamic constant linked to the free energy of adsorption, q_e (mg/g) the quantity of MB adsorbed per unit mass of adsorbent at equilibrium and q_m (mg/g) the quantity of dye adsorbed per gram material required to cover the surface of the adsorbent with a monomolecular layer or maximum adsorption capacity. C_e (mg/L) represents the residual concentration of MB at equilibrium.

The values of the parameters of the Langmuir and Freundlich models obtained after plotting the curves are grouped together in Table 3. The data fit well to the Langmuir model as shown in Table 3 with correlation coefficients (R^2) in the range 0.9935–0.9978, and maximum adsorption capacity of AC and MG-AC being 12.95 and 8.32 mg/g respectively. According Freundlich model, the heterogeneity factor n between 0.5 and 1 indicated that the adsorption of MB in water was favorable (Urbain et al., 2015).

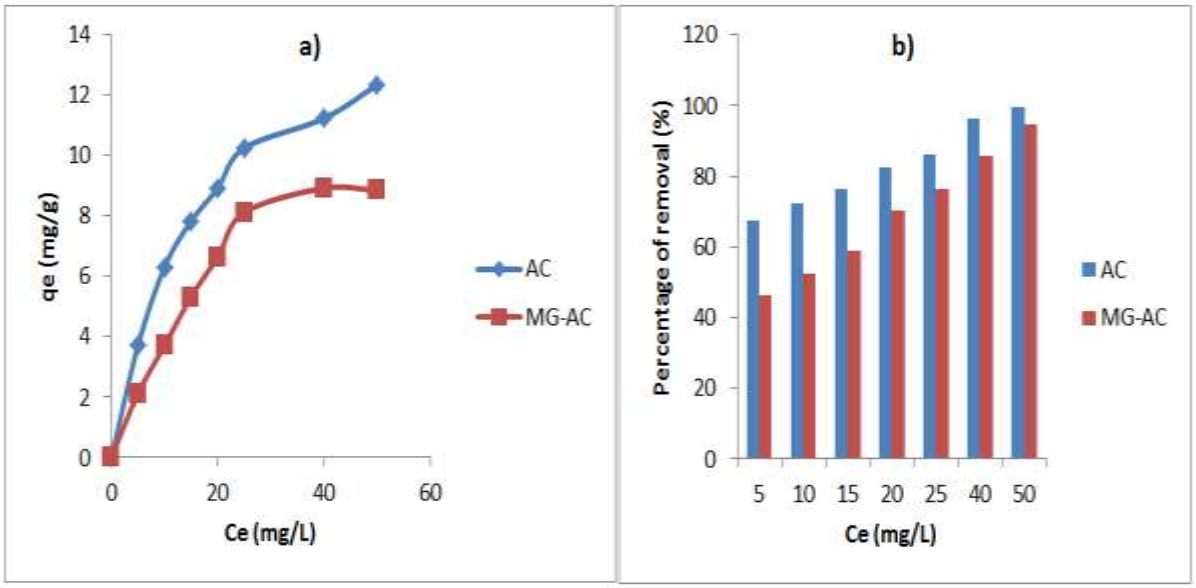

Figure 8:- a)MB adsorption isotherm on AC and MG-AC, percentage of MB removal by AC and MG-AC

Table 3:- Adsorption isotherm parameters for MB adsorption onto AC and MG-AC.

Model / Material	Langmuir			Freundlich		
	R^2	qm (mg/g)	b	R^2	lnK_F	1/n
AC	0.9978	14.05	0.0567	0.9569	1.8511	0.5063
MG-AC	0.9935	10.32	0.0267	0.9391	0.8479	0.6487

Methylene blue removal by heterogeneous Fenton

The heterogeneous Fenton process is an oxidation reaction based on the production of hydroxyl radicals from the reaction between iron ions and hydrogen peroxide (Vanessa et al., 2019, Sunet al., 2021). It is therefore these radicals that will greatly contribute to the degradation of MB. The equations of the reactions reflecting the mechanism are:

$$F_e^{2+} + H_2O_2 \rightarrow F_e^{3+} + OH^- + OH^{\bullet} k_1 = 76\ Ms^{-1} \textbf{\{1\}}$$

$$F_e^{3+} + H_2O_2 \rightarrow F_e^{2+} + HO_2^{\bullet} + H^+ k_2 = 0.001 - 0.01\ Ms^{-1} \textbf{\{2\}}$$

Figure 9 shows the elimination of methylene blue by theheterogeneous Fenton (adsorption-Fenton process coupling). MB elimination is greater with MG-AC. In addition, equilibrium is expected more quickly (60 min). Indeed, the iron particles of MG-AC will react with the peroxide to form hydroxyl radicals ($OH^{\bullet}$) which will contribute to the degradation of MB Christos et al., 2015). The addition of hydrogen peroxide in the solution containing only AC has very little influence on the equilibrium time and the adsorption mechanism.

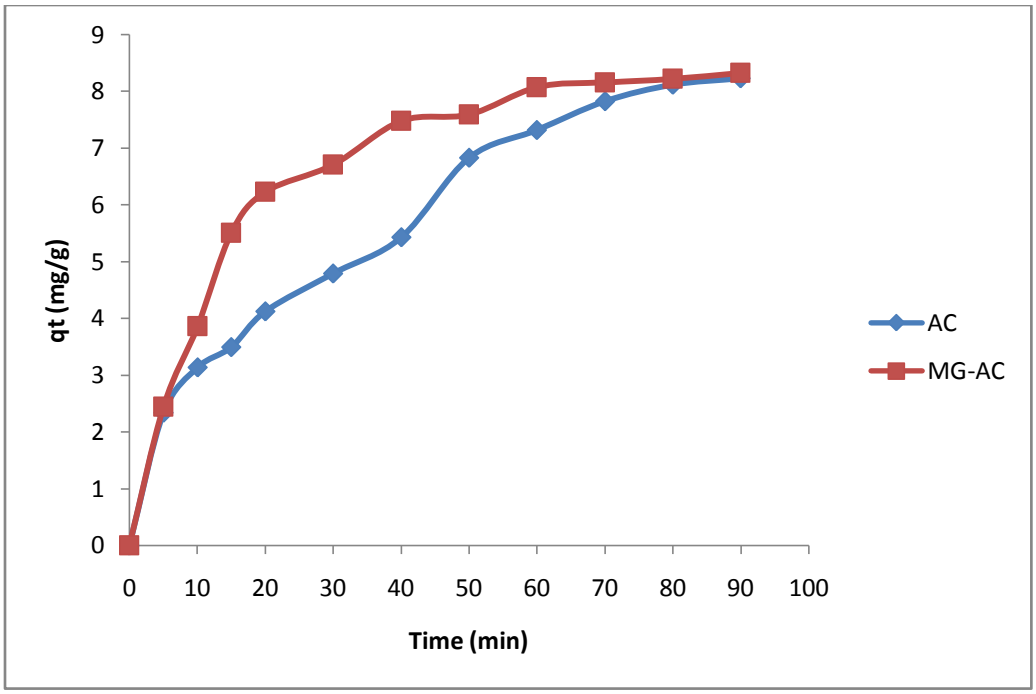

Figure 9:- Amount of MB removal in presence of H_2O_2 as a function of time (Conditions: mass of AC = mass of MG-AC= 0.1 g; T = 25°C).

Comparison of the two elimination mechanisms

The adsorption capacity of the materials according to the process used is presented in Figures 10. In the absence of hydrogen peroxide, AC adsorbs the MB molecule more than MG-AC. Indeed, the presence of iron oxide on the surface of the material prevents the fixation of methylene blue (Fig 10a). After adding hydrogen peroxide to the methylene blue solution in the presence of each of the materials, degradation is faster with MG-AC thanks to the release of powerful hydroxyl radicals (Fig 10b). For the solution containing activated carbon, the addition of hydrogen peroxide hardly contributes to the degradation. Indeed there is an adsorption competition between the molecules of H_2O_2 and those of MB (Xiaoming et al., 2018). The maximum amount of MB adsorbed on the materials according to the process is listed in Table 4. The adsorption/Fenton coupling is the most effective for removing methylene blue from water.

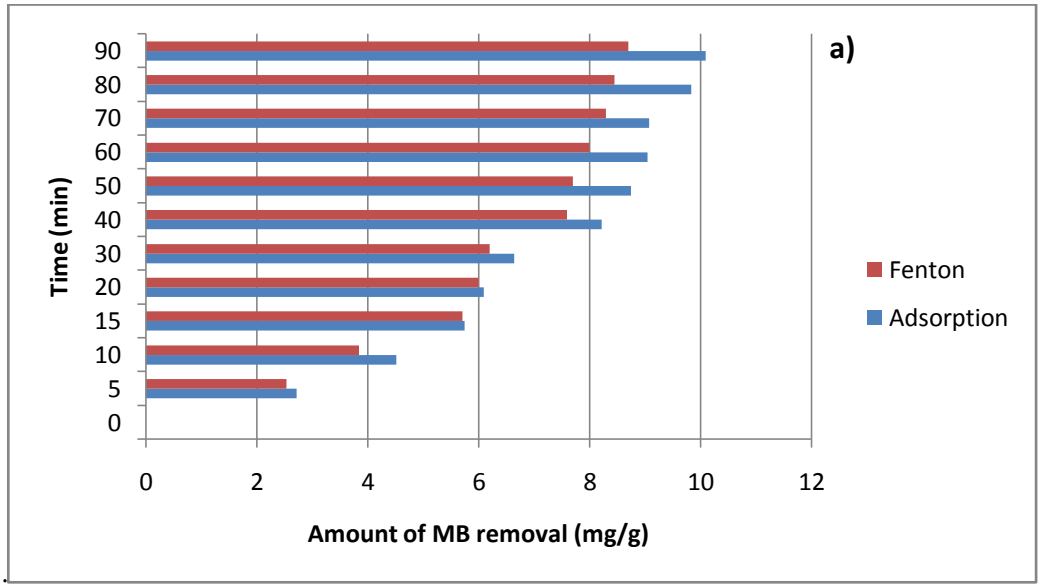

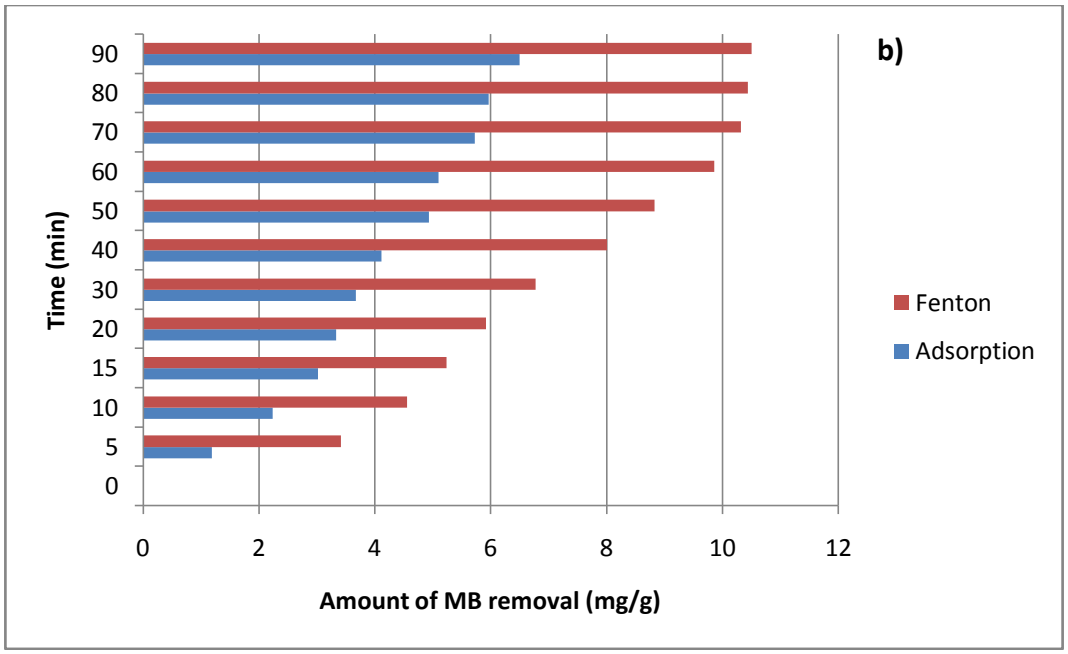

Figure 10:- Evolution of the quantity of MB eliminated by a) AC and b) by MG-AC.

Table 4:- Maximum amount of MB removed per mass of materials at equilibrium.

	AC	MG- AC
	Qm (mg/g)	Qm (mg/g)
With H_2O_2 (Fenton)	10.03	13.68
Without H_2O_2 (Adsorption)	13.40	9.60

The comparison of the adsorption capacity of these materials is grouped in Table 5. It can be seen that the results obtained are promising.

Table 5:- Adsorption capacities of different adsorbent for the removal of MB from wastewater.

Adsorbent	**Maximum adsorbent capacity, q_{max}(mg.g^{-1})**	**References**
Bio-char from pyrolysis of wheat straw	12.03	Liu et al., 2012
Activated carbon	8.77	Ijagbemi et al., 2010
Rice husk coir pith carbon	5.87	Kavitha et al., 2007
Activated desert plant	23	Bestani et al., 2008
MG-AC	9.60	This study
RicinodendronHeudelotii shells AC	13.40	This study

Material Performance and Stability

The stability of the synthesized materials was evaluated by carrying out the adsorption of MB following several cycles.It consisted of the Reusability of materials after desorption of MB and reprocessing. The stability results are shown in Figure 11. It can be seen that the percentage of MB degradation is decreasing for the two materials during the 4 cycles. We note, in a general way, that the percentage of degradation of the BM is decreasing for all the materials during the 4 cycles. The removal rate of MB is 99.4% and 94.6% respectively for AC and MG-AC. This elimination rate is greater than 90% in the 2nd cycle and decreases sharply in the 3rd cycle. It can be seen that in the third cycle, the MG-AC performs better than the AC. Despite a high mass (nearly 80% of mass recovered), the AC becomes less efficient. Desorption combined with heat treatment seems less and less effective. In the 4th cycle, the percentage elimination of MB is greater than 68 % for MG-AC and is equal to 5.23% for AC. This is due to a more considerable mass loss of the mass of activated carbon during the various cycles, in particular for the 4th cycle (30% of mass recovered). Indeed, the recovery of activated carbon is more difficult than MG-AC whose regeneration is easy, due to its magnetic properties.Due to the low elimination rate of MB in the 4th cycle and the low mass of AC

recovered, it is difficult to continue the tests. This result is in agreement with the results of some authors who easily recovered magnetic activated carbons and reused them with good results (Seyedehmaryamet al., 2020, Gupta et al., 2012).The MG-AC performs well over multiple cycles.

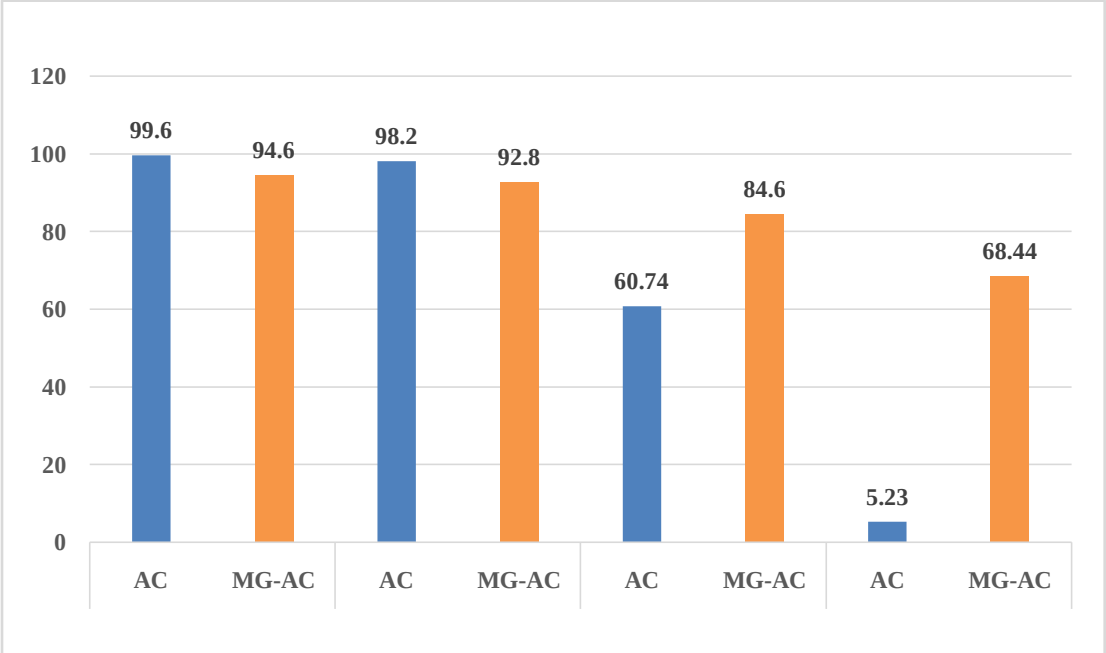

Figure 11:- Evolution of the percentage of MB elimination during the 4 cycles

Conclusion:-

This study focused on the synthesis of carbonaceous and carbonaceous-ferromagnetic material based on RicinodendronHeudelotii for its use to remove methylene blue dye. The activated carbon obtained is microporous. The reaction of iron II and iron III ions with the prepared carbon gave a magnetic carbon with the presence of iron oxide Fe_2O_3 at 86.5%. These materials have heterogeneous surfaces. Adsorption of methylene blue by AC and MG-AC is pseudo second order with an equilibrium time of 90 min. This dye adsorbs more on AC than on MG-AC whose presence of iron oxide does not allow the molecules to adsorb easily. The Langmuir model can be used to describe this adsorption phenomenon with maximum adsorption amounts of 13.4 and 9.6 mg/g respectively for AC and MG-AC. The iron ions present in MG-AC react with H_2O_2 to release radicals which will contribute to increasing the elimination power of this material. In addition MG-AC is stable and efficient in the elimination of methylene blue over 4 cycles.

Acknowledgment:-

The authors thank the Central Laboratory of the University of Man for the material

References:-

1. Abo E.A., Kouakou Y.U., Yobouet Y.A., Trokourey A., 2021. Adsorption of Remazol Black 5 and Indigo Carmine on Corn Cobs Activated Carbon: Kinetic, Equilibrium, and Thermodynamic Studies. Indian Journal of Advances in Chemical Science, 9 (2), 69-75.
2. Ammar A.B., Basma A.B., Atheer M.A.Y., Mohanad K.M., Zainab S.A.H., 2022. Color Removal of Textile Wastewater Using Electrochemical Batch Recirculation Tubular Upflow Cell. International Journal of Chemical Engineering, 2022, 1-8.
3. Bestani B., Benderdouche N., Benstaali B., Belhakem M., Addou A., 2008. Methylene blue and iodine adsorption onto an activated desert plant. Bioresource Technology, 99, 8441–8444.
4. Boujaady H.E., Mourabet M., Ziatni M.B., Taitai A., 2013. Adsorption/desorption of direct yellow 28 on apatitic phosphate: Mechanism, kinetic and thermodynamic studies. Journal of the Association of Arab Universities for Basic and Applied Sciences,14, 1-11.

5. Chinedum A., Nur A.M.A., Zaiton A.M., Adibah Y., Jafariah J., 2017. Nanotechnology Environmental Engineering, 2(16), 1-25.
6. Christos D.G., Henry J.S., Christopher P.M., Konstantinos G., Ioannis P., 2015. Evidence for photochemical production of reactive oxygen species in desert soils. Nature Communications, 6, 1-11.
7. Francesca B., Roberto D.G., Antonell P., Michela S., 2019. Efficiency in waste management companies: A proposal to assess scale economies. Resources, Conservation and Recycling, 148,124-131.
8. Gupta V.K., Arunima N., 2012. Cadmium removal and recovery from aqueous solutions by novel adsorbents prepared from orange peel and Fe_2O_3 nanoparticles. Chemical Engineering Journal,180, 81- 90.
9. Ho Y.S., McKay G., 1999. Pseudo-second order model for sorption processes. Process Biochemistry, 34, 451-465.
10. Ijagbemi C.O., Chun J.L., Han D.H., Cho H.Y., Kim D.S., 2010. Methylene Blue adsorption from aqueous solution by activated carbon: Effect of acidic and alkaline solution treatments. Journal of Environmental Science and Health, Part A, 45, 958–967.
11. Kambiré O., Kouakou Y.U., Kouyaté A., Sadia S.P., Kouadio K.E., 2021. Removal of rhodamine B from aqueous solution by adsorption on corn cobs activated carbon. Mediterranean Journal of Chemistry, 11(3), 271-281.
12. Kavitha D., Namasivayam C., 2007. Experimental and kinetic studies on methylene blue adsorption by coir pith carbon. Bioresource Technology, 98, 14–21.
13. Khu L.V., Thu T.T., 2014. Activated carbon derived from rice husk by NaOH activation and its application in supercapacitor. Progress in Natural Science: Materials International, 24(3), 191-198.
14. Kouakou Y.U., Abo E.A., Yobouet Y.A., Trokourey A., 2022. Kinetic and thermodynamic study of the adsorption of methylene blue on activated carbon based on corn cobs. Journal of Materials and Environmental Science, 13(4), 367-381.
15. Kouakou Y.U., Essy K.F., Dembélé A., Brou Y.S., Ello S.A., 2017. Removal of imidacloprid using activated carbon produced from Ricinodendronheudelotii shells. Bulletin of the Chemical Society of Ethiopia, 31(3), 397-409.
16. Kristina Plenderleith. RıcınodendronHeudelotııA State of Knowledge Study undertaken for the Central African Regional Program for the Environment. Oxford Forestry Institute Department of Plant Sciences University of Oxford United Kingdom. (1997)
17. Liu Y., Zhao X., Li J., Ma D., Han R., 2012. Characterization of bio-char from pyrolysis of wheat straw and its evaluation on methylene blue adsorption. Desalination and Water Treatment, 46, 115–123.
18. Luiz C.A.O., Elaine P., Iara R.G., Andrea V., Márcio P., 2009. Preparation of activated carbons from coffee husks utilizing $FeCl_3$ and $ZnCl_2$ as activating agents. Journal of Hazardous Materials, 165, 87-94.
19. Mahmoud T., Nassima B., Salem B., Hassina G., 2014. Préparation et caractérisation d'un charbon actif à partir de la coquille d'amande (Prunus amygdalus) amère. Biotechnologie, Agronomie, Société et Environnement, 18(4), 492-502 .
20. Manoel V.B.G., Stela C.D.O., Bruna M.P.N.A., Elidia M.G., Dane T.C., 2016. Electrocoagulation/electroflotation process applied to decolourization of a solution containing the dye yellow sirius. International Journal of Electrochemical Science, 11, 7576–7583.
21. Marina C.B., Ruben L.L., Fatima S.G., Ruben E.G., 2021. Effective use of activated carbon from olive stone waste in the biosorption removal of Fe(III) ions from aqueous solutions. Journal of Cleaner Production, 294, 1-14.
22. Muslem M., Agus K., Taffrika N.H., Roto R., 2019. Preparation of Char-Fe_3O_4 Composites from Polyvinyl Chloride with Hydrothermal and Hydrothermal-Pyrolysis Carbonization Methods as Co(II) Adsorbents. Indonesia Journal Chemistry, 19(4), 835- 840.
23. Oualid H., Emmanuel N., 2007. Modeling of adsorption isotherms of phenol and chlorophenols onto granular activated carbon Part I. Two-parameter models and equations allowing determination of thermodynamic parameters. Journal of Hazardous Materials, 147, 381–394.
24. Panagiota P., Dimitrios K., Evan D., 2008. Review Production of activated carbon from agricultural by-products. Journal of Chemical Technology and Biotechnology,83, 581-592.
25. Seyedehmaryam M., Chin W.L., Sinyee G., Golnoush Z., Omid A.P., Mohd R.J., 2020. Application of Efficient Magnetic Particles and Activated Carbon for Dye Removal from Wastewater. ACS Omega, 5, 20684−20697.
26. Sudheer K.S., Noof R.S.A.M., Hajar M.A.S., Keunje Y.H.A.S., 2020. Low-cost activated carbon production from organic waste and its utilization for wastewater treatment. Applied Water Science volume, 10(6), 1-9.
27. Süheyda A., Gülin E., 2015. Advanced Oxidation Processes for Removal of Dyes from Aqueous Media.Green Chemistry for Dyes Removal from Wastewater, (83–117). 2015. http://dx.doi.org/10.1002/9781118721001.ch3

28. Sun H., Yao Y., Wei F., Zhao Q., Liu B., Zhang L., 2021. Process optimization and mechanism study of acid red G degradation by electro-FentonFeox process as an in situ generation of H_2O_2. Turkish Journal of Chemistry, 45, 5-16.
29. Suphitcha W,.Sayam A, Patana T., Acharaporn K., Suntree S., 2013. Removal of Reactive Dyes from Textile Dyeing Industrial Effluent by Ozonation Process. APCBEE Procedia 5, 279-282.
30. Urbain K., Aimé S.E., Jacques A.Y., Albert T., 2013. Adsorption of iron and zinc on commercial activated carbon. Journal of Environmental Chemistry and Ecotoxicology, 5(6), 168-171.
31. Urbain P.G., Koffi M.Y., Brou L.Y., Aka M.K., Ardjouma D., 2015.Adsorption du benzo(a)pyrène sur du charbon activé à base de coques de coco provenant de Côte d'Ivoire. International Journal of Biological and Chemical Sciences, 9(5), 2701-2711.
32. Vanessa G., Marco S.L., José A.P., 2019. Combination of adsorption and heterogeneous photo-Fenton processes for the treatment of winery wastewater. Environmental Science and Pollution Research International , 26(30), 31000-31013.
33. Water V.R., Sangeetha S., Vairam S., 2014. Synthesis of magnetic activated carbon/α-Fe_2O_3nanocomposite and its application in the removal of acid yellow 17 dye from water. Journal of Hazardous Materials, 273, 127-135.
34. Xiaoming P., Fengping H., Tao Z., Fengxian Q., Hongling D., 2018. Amine functionalized magnetic bamboo-based activated carbon adsorptive removal of ciprofloxacin and norfloxacin: A batch and fixed-bed column study. Bioresource Technology, 249, 924-934.
35. Yanhui L., Qiuju D., Tonghao L., Xianji P., Junjie W., 2013. Comparative study of methylene blue dye adsorption onto activated carbon, graphene oxide, and carbon nanotubes. Chemical Engineering Research and Design, 91, 361-368.